



EDITOR'S CHOICE

Random walk model simulates the increased drowsiness of children with obstructive sleep apnea

To cite this article: Shu Guo *et al* 2020 *EPL* **129** 60002

View the [article online](#) for updates and enhancements.

You may also like

- [Actigraphy combined with EEG compared to polysomnography in sleep apnea patients](#)
Ingo Fietze, Thomas Penzel, Markku Partinen et al.
- [Decreased sample entropy during sleep-to-wake transition in sleep apnea patients](#)
Xueyu Liang, Jinle Xiong, Zhengtao Cao et al.
- [Interbeat interval-based sleep staging: work in progress toward real-time implementation](#)
Gary Garcia-Molina and Jiewei Jiang

Random walk model simulates the increased drowsiness of children with obstructive sleep apnea

SHU GUO¹, HILA DVIR², SHLOMO HAVLIN², DAQING LI^{3,1(a)}, RUI KANG^{1,4} and RONNY P. BARTSCH²

¹ School of Reliability and Systems Engineering, Beihang University - Beijing 100191, China

² Department of Physics, Bar-Ilan University - Ramat Gan, Israel

³ Beijing Advanced Innovation Center for Big Data-Based Precision Medicine, Beihang University Beijing 100191, China

⁴ National Key Laboratory of Science and Technology on Reliability and Environmental Engineering Beijing 100191, China

received 6 February 2020; accepted in final form 2 April 2020
published online 10 April 2020

PACS 05.40.Fb – Random walks and Levy flights

PACS 05.40.-a – Fluctuation phenomena, random processes, noise, and Brownian motion

PACS 87.10.Mn – Stochastic modeling

Abstract – Obstructive sleep apnea (OSA) is a common sleep disorder, which is particularly harmful to children as it may lead to learning deficits, attention deficit hyperactivity disorder (ADHD) and growth retardation. Furthermore, OSA alters the dynamics of sleep-stage transitions and in particular increases the transition time from being awake to falling asleep (“drowsiness”). In this letter, we show that sleep bout durations during this transient state can be described by an exponential distribution with a longer characteristic time scale for OSA compared to healthy children. This finding can be simulated and better understood by using a random walk model of the integrated neuronal voltage of wake-promoting neurons, and by introducing a new concept of a light sleep threshold parameter L that distinguishes between drowsiness and deeper forms of light sleep. Our analysis also shows that the value of L correlates well with OSA severity. Moreover, we find that after OSA treatment, the parameter L returns to normal values similar to those we detected for healthy children. We anticipate that our methodology can help in better understanding and modeling sleep dynamics, and may improve diagnostics and treatment monitoring of OSA.

 Copyright © EPLA, 2020

Introduction. – Human sleep is characterized by rapid eye movement (REM) sleep as well as by light and deep sleep (non-REM). In addition, sleep is often interrupted by brief awakenings (arousals) that last from few seconds to minutes [1,2]. Most of the modeling approaches to sleep focus on the diurnal and circadian sleep/wake cycle [3–8], and models based on flip-flop switches were developed to account for the transitions between sleep and wake state as well as between REM and non-REM sleep [8–10]. There have been a few studies analyzing the probability distributions of arousal durations during sleep revealing a power-law behavior [1,11,12], which is consistently observed for several mammalian species [13] and seems to be related to different stages of maturation [14,15]. First attempts to simulate the sleep microarchitecture and the underlying

power-law in arousal durations utilize stochastic and random walk based models [1,16], however, the complex dynamics of sleep-stage transitions and their alteration with sleep disorders such as obstructive sleep apnea (OSA) is not yet understood.

In this letter, we focus on non-REM sleep transitions and changes in their dynamics that possibly occur in children with OSA. Here, we propose a new parameter L that is related to the depth of light sleep, and we show its utility in characterizing the severity of OSA. In the current guidelines of the American Academy of Sleep Medicine (AASM), non-REM sleep is divided into three stages according to sleep depth: stages N1 and N2 (light sleep) as well as stage N3 (deep sleep) [17]. The sleep stage N1 represents sleep in its lightest form and is therefore considered a transitional state between wakefulness and sleep. N1 sleep is characterized by drowsiness [18] during

(a)E-mail: daqingl@buaa.edu.cn (corresponding author)

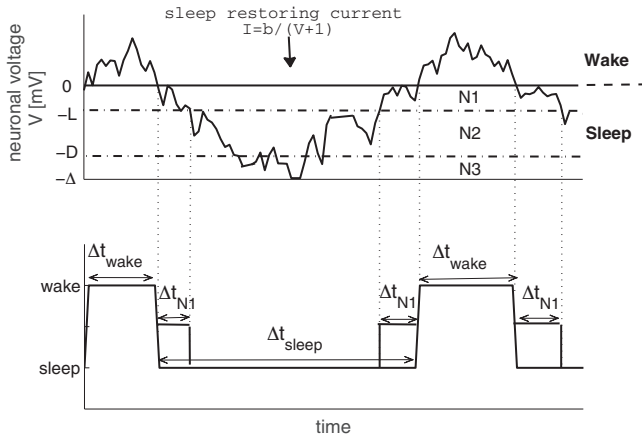


Fig. 1: Model of a random walk that simulates the integrated voltage of wake-promoting neurons (WPN). The upper panel illustrates the dynamics of the model: the neuronal voltage of WPN shows unbiased diffusion for negative values of V (corresponding to sleep), whereas for positive values of V arousals occur and diffusion is biased towards sleep due to a sleep restoring current [1,12]. In our model, sleep is further divided into three stages according to the neuronal voltage: light sleep stages N1 (for $0 \leq V < -L$) and N2 (for $-L \leq V < -D$) as well as deep sleep N3 (for $-D \leq V \leq -\Delta$) [16]. The lower panel shows the derived hypnogram from the simulated neuronal voltage dynamics. N1 sleep bout durations are marked as Δt_{N1} in the lower panel.

which individuals usually respond to auditory or visual stimuli [19]. The N1 stage accounts for only a small portion of the total sleep time (TST), and therefore has often been ignored or grouped together with stage N2 into a single light sleep stage [20,21]. However, since N2 is more dominant (>50% of TST) than N1 (<10% of TST) [22], combining N1 with N2 might abolish any N1 effects that are related, for example, to cognitive performance. Indeed, very recent studies have shown a relationship between N1 (but not N2) percentage and cognitive impairment. Specifically, high percentage of N1 was found to be a good predictor of declining cognitive function in elderly subjects [23,24]. Additionally, it has been shown that N1 percentage increases for OSA patients (for both adults [25–27] and children [28,29]), whereas no difference has been found for N2 [25,30]. Furthermore, for children, OSA and sleep-disordered breathing in general, have been linked to hyperactivity [31] and poor school performance [32,33], and timely diagnosis and treatment of OSA can lead to immediate improvements [34,35]. In this work we focus on N1 sleep bout durations (Δt_{N1}), and based on a statistical physics model, we derive N1 sleep characteristics that can aid in better understanding sleep in OSA patients.

Recently, a model has been developed to simulate brief arousals from sleep [12,16]. The model is based on a physiological mechanism that takes into account the intrinsic noise (“sub-threshold voltage fluctuations”) of

wake-promoting neurons (WPN) in the brain stem. Although WPN are suppressed during sleep [10,36], the integrated uncorrelated neuronal noise from WPN can from time to time cross the excitability threshold and through projections to the cortex provoke an arousal. Because of the excitation along the ascending arousal pathway, sleep-promoting neurons (SPN) in the ventrolateral (VLPO) and median (MnPO) preoptic nuclei are stimulated [37,38], and can in turn actively inhibit the WPN (negative feedback) through an inhibitory current [12]. The integrated voltage $V(t)$ of WPN can be modeled as a random walk with drift (during arousals/short awakenings) or without drift (during sleep) as shown in fig. 1. During sleep, the random walker transitions through the different non-REM sleep stages, and in order to quantify the probability of $V(t)$ being in a state corresponding to N1, here we introduce a threshold L (fig. 1) that distinguishes between shallow and deeper light sleep, N1 ($0 \leq V < -L$) and N2 ($-L \leq V < -D$) light sleep, respectively. In the following, we propose an analytical method to evaluate L from standard sleep recordings (hypnograms), and we determine L for healthy children and children with OSA. We find that OSA yields higher values of L that can be reduced through proper treatment.

Data. – We analyze hypnograms of two groups of children that are age- and BMI-matched: i) healthy children ($n = 38$; age: 6.7 ± 1.9 years; BMI: 17.7 ± 4.3 kg/m²), and ii) OSA children ($n = 58$; age: 6.5 ± 2.3 years; BMI: 18.6 ± 5.0 kg/m²). In addition, we analyze the hypnograms of $n = 9$ children that received successful OSA treatment of either CPAP or surgery (age: 7.5 ± 2.3 , BMI: 18.1 ± 5.8 kg/m²). Hypnograms were scored in 30 s epochs [17] and contain the following stages: wakefulness, REM sleep, and non-REM sleep stages N1, N2 and N3.

Calculating the threshold L from N1 sleep bout durations. – During sleep, the random walker transitions freely through the non-REM sleep stages N1, N2 and N3 (fig. 1), and changes in the integrated neuronal voltage $V(t)$ of WPN can be calculated by the following differential equation:

$$dV = \sigma \cdot dw, \quad \text{for } -\Delta \leq V \leq 0, \quad (1)$$

where σ is the standard deviation of the neuronal voltage fluctuations, w is a standard Wiener process, and $-\Delta$ is the relative voltage value between threshold potential and potassium Nernst potential [12]. To model the probability distribution of Δt_{N1} , we introduce a N1 light sleep threshold, L , so that, for voltages between 0 and $-L$, N1 sleep occurs (fig. 1). In the following, we show how to estimate L from standard hypnogram data.

During N1 light sleep, the voltage is bounded within $-L \leq V \leq 0$ (fig. 1). Therefore, integrating eq. (1) in this range yields

$$0 - (-L) = \sigma \cdot \int dw \quad (2)$$

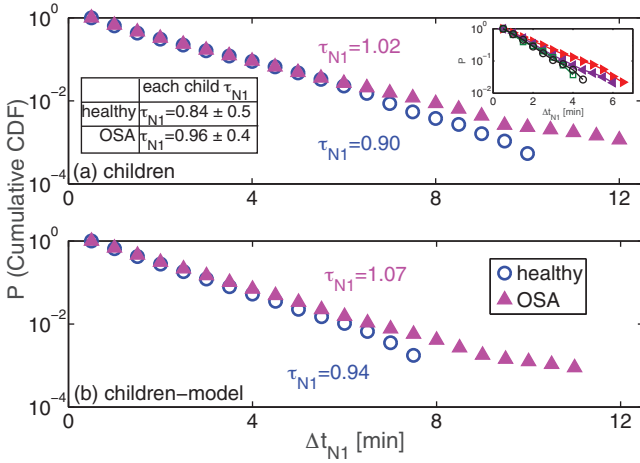


Fig. 2: Cumulative probability distributions of N1 sleep bout durations (Δt_{N1}) decay exponentially. (a) OSA leads to a slight increase of the Δt_{N1} characteristic time constant τ_{N1} (healthy children (blue open circles) *vs.* OSA children (magenta filled triangles)). Panel (b) shows the corresponding results of our model simulations (fig. 1) for both children groups. The distributions in both panels are obtained from the pooled data of each group, and the characteristic time constants τ_{N1} are calculated using maximum-likelihood estimation (MLE) of exponential distributions (eq. (9)), which does not depend on specific bin selection for the probability distribution. The inset table in panel (a) shows the τ_{N1} values (mean \pm standard deviation) for healthy and OSA children, obtained by averaging the individual τ_{N1} values of each child of the corresponding group. As typical examples, in the inset figure of panel (a) we present the cumulative probability distribution of two healthy children (open symbols) and two children with OSA (full symbols), all of which show approximately exponential distributions (close to straight lines on a semi-log plot). The model results for each group (healthy and OSA) were obtained from 50 independent simulations with length of 10 hours each. The model parameters for each group were adjusted according to the empirical findings. For healthy children: $L = 5$, neuronal noise parameter $\sigma = 5.7$, sleep inertia parameter $b = 25$, sleep depth parameter $\Delta = 25$. For OSA children: $L = 6$, $\sigma = 6.3$, $b = 30$, $\Delta = 25$. The values for L are taken from the results presented in fig. 3; b and σ are determined by $b = \sigma^2 \cdot f(\alpha)$ and $\sigma = \Delta / \sqrt{\tau_{\text{sleep}}}$, respectively, with $\Delta = 25$ for both groups (for more details, see [16]). The exponent τ_{sleep} is obtained from the probability distribution of sleep bouts of each child [12]. Since the model assumes an exponential distribution of Δt_{N1} and the simulations were performed using the L as observed from the sleep data (see fig. 3), the close resemblance of empirical and model data supports our hypothesis of a light sleep threshold and of an approximately exponential distribution of Δt_{N1} . Note that we apply cumulative CDF in order to reduce the noise in the data.

or

$$L^2 = \sigma^2 \cdot \left(\int dw \right)^2. \quad (3)$$

Since the differentials dw of a Wiener process are uncorrelated and have zero mean, averaging eq. (3) over all N1

sleep bouts yields

$$L^2 = \sigma^2 \cdot \int \langle (dw)^2 \rangle, \quad (4)$$

$$L^2 = \sigma^2 \cdot \int dt, \quad (5)$$

$$L^2 = \sigma^2 \cdot \tau_{N1}. \quad (6)$$

In the step from eq. (4) to eq. (5), we use a property of w (standard Wiener process) that the variance of dw is the time interval dt of the process, and therefore τ_{N1} (in eq. (6)) is the average duration of an N1 sleep bout. Thus, for the N1 light sleep threshold we obtain

$$L = \sqrt{\tau_{N1}} \cdot \sigma. \quad (7)$$

As seen in fig. 2, we find that the probability distribution of Δt_{N1} decays exponentially as

$$P(\Delta t_{N1}) \propto \exp[-(\Delta t_{N1})/\tau_{N1}], \quad (8)$$

and the characteristic time constant τ_{N1} equals the inverse slope of the probability distribution of Δt_{N1} on a semi-log plot (fig. 2). The standard deviation of the neuronal voltage fluctuations σ can be thus calculated by using the characteristic time constant τ from all sleep bout durations: $\sigma = \Delta / \sqrt{\tau}$ with $\Delta = 25$ mV for children and $\Delta = 23$ mV for adults (for details on how to derive σ and Δ , see [16]).

Estimating the characteristic time constant Δt_{N1} from N1 sleep bout durations. – The probability distribution of Δt_{N1} decays exponentially with characteristic time constant τ_{N1} (fig. 2 and eq. (8)) that can be calculated using the maximum likelihood estimation (MLE) [12,39]. An advantage of MLE analysis is its independence from a specific bin selection of the probability distribution.

The exponential probability distribution of N1 sleep bout durations can be approximated as $f(\Delta t_{N1}) = 1/\tau_{N1} \cdot \exp[-(\Delta t_{N1} - M)/\tau_{N1}]$, where Δt_{N1} is the variable of the N1 sleep bout durations, and M is the shortest value of Δt_{N1} . The likelihood ℓ for the data (with N variables) is

$$\begin{aligned} \ell &= \prod_{i=1}^N \left(\frac{1}{\tau_{N1}} \cdot \exp[-(\Delta t_{N1}^i - M)/\tau_{N1}] \right), \\ \ell &= \left(\frac{1}{\tau_{N1}} \right)^N \cdot \exp \left[\sum_i -(\Delta t_{N1}^i - M)/\tau_{N1} \right], \\ \ln \ell &= -N \cdot \ln \tau_{N1} - \frac{\sum_i (\Delta t_{N1}^i - M)}{\tau_{N1}}, \end{aligned}$$

and the maximum of ℓ is attained when $d(\ln \ell)/d\tau_{N1} = 0$:

$$\frac{d(\ln \ell)}{d\tau_{N1}} = 0 = -\frac{N}{\tau_{N1}} + \frac{\sum_i (\Delta t_{N1}^i - M)}{(\tau_{N1})^2}.$$

Therefore, the estimated value for τ_{N1} is (as expected for exponential distributions)

$$\hat{\tau}_{N1} = \frac{\sum_i (\Delta t_{N1}^i - M)}{N} = \langle \Delta t_{N1} - M \rangle. \quad (9)$$

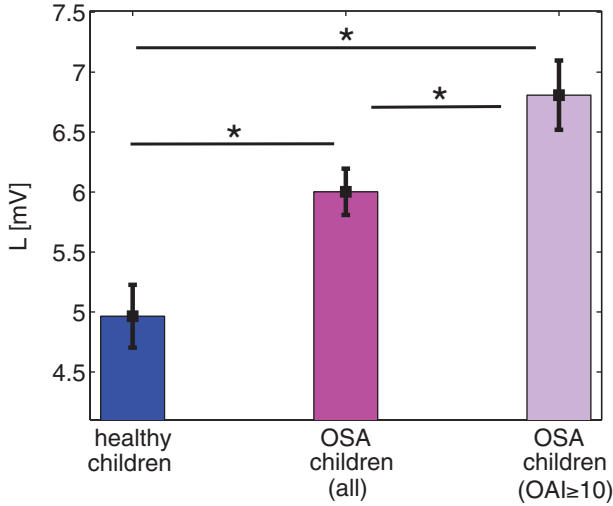


Fig. 3: The N1 light sleep threshold L for different groups of children. The L values are calculated for each individual utilizing eq. (7), and averaged for each group. OSA children have higher values of L as compared to healthy ones, which increase even further for children with severe OSA (Obstructive Apnea Index (OAI) ≥ 10 events/hour [34], $n = 12$). The higher L values for OSA children may explain their longer N1 and shorter N2 light sleep (upper panel in fig. 1). Shown are mean and standard deviation for each group. Significant differences between the groups were probed by Mann-Whitney U tests and * indicates significant differences with $p < 0.05$. For the calculation of L we use maximum likelihood estimation (MLE) (eq. (9)) with $M = 1$ min for all children groups.

Here, $\hat{\tau}_{N1}$ was calculated from the Δt_{N1} data in the interval [1 min, 10 min], therefore, $M = 1$ min in eq. (9).

Using the Cramér-Rao bound [40], the estimated error of τ_{N1} is

$$\begin{aligned} J_{\tau_{N1}} &= - \left\langle \frac{d^2(\ln \ell)}{d(\tau_{N1})^2} \right\rangle \\ &= - \left\langle \frac{N}{(\tau_{N1})^2} - 2 \cdot \frac{\sum_i (\Delta t_{N1}^i - M)}{(\tau_{N1})^3} \right\rangle \\ &= - \frac{N}{(\tau_{N1})^2} + 2 \cdot \frac{N \cdot \tau_{N1}}{(\tau_{N1})^3} = \frac{N}{(\tau_{N1})^2} \approx \frac{N}{(\hat{\tau}_{N1})^2}, \end{aligned}$$

where $J_{\tau_{N1}}$ is the Fisher information of τ_{N1} . Therefore, the lower bound of the standard deviation of τ_{N1} is

$$\sigma_{\tau_{N1}} = \sqrt{\frac{1}{J_{\tau_{N1}}}} = \frac{\hat{\tau}_{N1}}{\sqrt{N}}. \quad (10)$$

Results. – Figure 2 shows the cumulative probability distributions of Δt_{N1} for the healthy children and for the OSA group on semi-log plots. The cumulative distribution function is defined as $\text{CDF} \equiv \int_{\Delta t_{N1}}^{\infty} f(r) dr$, where $f(\Delta t_{N1})$ is the probability density function for the occurrence of sleep stage N1 with duration Δt_{N1} . Both distributions decay approximately exponentially with Akaike weights [41] for an exponential distribution > 0.9 and for

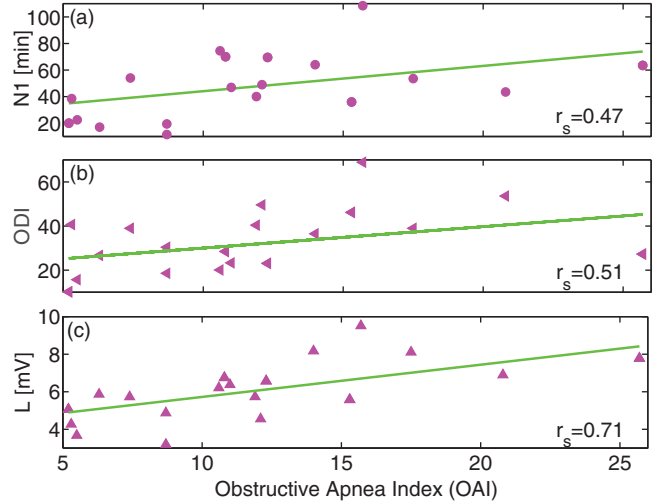


Fig. 4: Spearman's rank correlation between different sleep characteristics and Obstructive Apnea Index (OAI) for OSA children. (a) The N1 sleep duration increases with the severity of OSA as measured by OAI (Spearman $r_s = 0.47$). (b) A similar correlation with $r_s = 0.51$ is found for oxygen desaturation events (a traditional diagnostic marker of sleep apnea severity measured by the oxygen desaturation index (ODI)). (c) Plot of the value of L as a function of OAI of each child reveals the strongest correlation to OAI among the three measures considered (Spearman $r_s = 0.71$). Therefore, the parameter L might be an even better indicator of OSA severity than N1 or ODI. For the analysis, we included all children with $\text{OAI} \geq 5$ (all moderate and severe cases of OSA [34]). Note that the correlations r_s in all panels (a)–(c) are of statistical significance with $p < 0.05$, *i.e.*, all correlations r_s are significantly different from zero. ODI is calculated from the number of events per hour where oxygen desaturation of 3% or more was associated with a respiratory event.

a power-law distribution < 0.1 . We find that the characteristic time constant τ_{N1} tends to be larger for OSA children, however, the difference is not statistically significant when comparing the values of each individual (see inset table in fig. 2(a)). Our model simulations result in probability distributions for Δt_{N1} similar to the empirically obtained distributions (see fig. 2(b)).

We next calculate the N1 light sleep threshold L from sleep bout distributions for each group according to eq. (7). Interestingly, although τ_{N1} values are not significantly different when comparing healthy to OSA children, the obtained values of L show significant differences as can be seen in fig. 3. We find that L is significantly larger for OSA children, particularly for severe cases of OSA (Obstructive Apnea Index (OAI) ≥ 10 events/hour [34]). We relate the higher values of L for OSA to the significantly longer N1 durations seen in those children [28,29].

Previous studies have found that N1 sleep duration increases under OSA [25,30]. For children, this N1 increase correlates with OSA severity, *i.e.*, children with higher OAI tend to have more N1 sleep (fig. 4(a)) [27,29]. The most important consequences of OSA, however, are

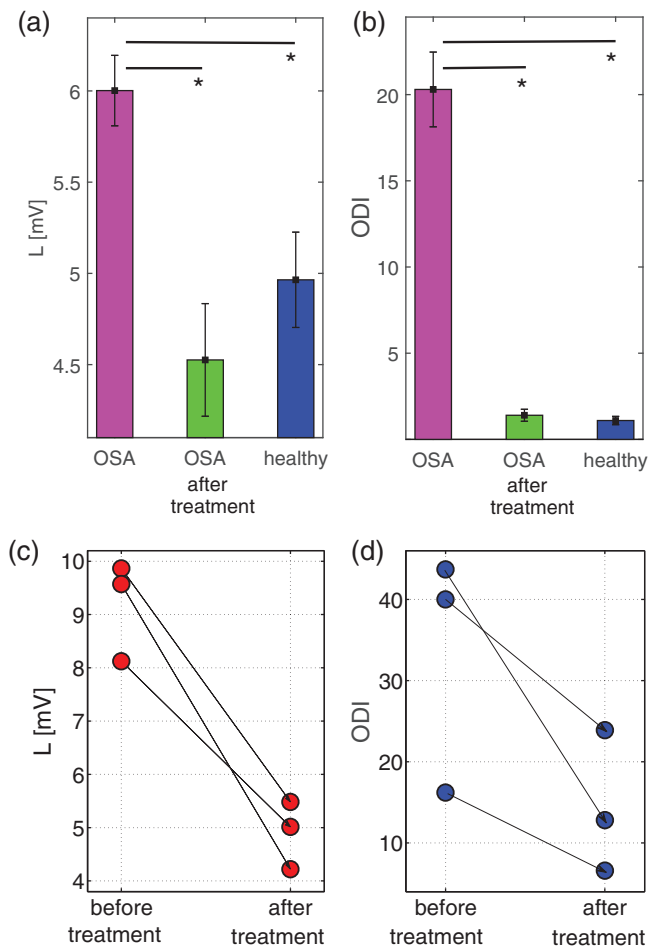


Fig. 5: The effect of treatment on N1 light sleep threshold L and oxygen desaturation index (ODI) for OSA children. (a), (b): while untreated OSA children show the highest L and ODI values, treatment with CPAP or surgery significantly lowers L and ODI values, which become close to those obtained for healthy children. (c) For $n = 3$ OSA children we have data before and after treatment, which clearly show a significant decrease in L after treatment ($p = 0.02$). This decrease is even more pronounced than the corresponding decrease in ODI for the same children (panel (d)), since it allows for a group separation (before/after treatment) on the basis of L but not ODI (the p -value for ODI is $p = 0.1$). Mann-Whitney U tests are applied to probe statistical significant differences between the group (* indicates significant differences for $p < 0.05$).

oxygen desaturation episodes and hypoxemia that cause a multitude of neuropathological changes and neuropsychological impairments [42]. These episodes are detected by a fingertip pulse oximeter usually in combination with a polysomnogram (PSG), and the average number of desaturations per hour is quantified by the oxygen desaturation index (ODI). Since ODI is sensitive to apnea depth and length, it can be used as a prognostic marker for OSA complications and mortality [43]. In our data of OSA children, ODI shows good correlation with OAI (fig. 4(b)), similar to what was found recently for OSA adults [44].

Interestingly, as we show in fig. 4(c), the N1 light sleep threshold L , a physiological parameter proposed here, can be used to evaluate OSA severity. Plotting L as a function of the patients OAI shows a strong correlation of 0.71 (fig. 4(c)) for moderate OSA ($5 \leq \text{OAI} < 10$) to severe cases of OSA ($\text{OAI} \geq 10$) [34]. This is an even higher correlation than what we find for N1 and ODI, indicating that L may be useful as a diagnostic marker of OSA. Moreover, calculating L only requires hypnograms and no additional device to measure oxygen desaturation (which is necessary to determine ODI).

The treatment of OSA in children includes a combination of medications (such as topical nasal steroids), a surgical removal of tonsils and adenoids (“adenotonsillectomy”), therapy with a CPAP mask during sleep and/or oral appliances (such as dental devices or mouthpieces to keep the upper airway open) [45]. In our study, treatment strategies were chosen based on the children’s clinical situation and each child’s family decision, and mostly included CPAP and adenotonsillectomy.

In fig. 5 we show the effect of treatment on the N1 light sleep threshold L . Compared to children with untreated OSA, those who underwent treatment by CPAP or surgery have significantly lower values of L . In fact, their L values become similar to healthy children (fig. 5(a)). Moreover, we can reinforce this observation of the decrease of L with treatment on individual basis. For $n = 3$ children we have obtained longitudinal data before and after treatment (with either CPAP or surgery) and we calculated the corresponding L values. It is clearly seen that treatment of these children lowered L significantly by 30–40% (fig. 5(c)) and ODI by more than 50% (fig. 5(d)). However, these preliminary results need to be confirmed by follow-up studies on a larger study cohort.

Conclusion. – Traditionally, obstructive sleep apnea is diagnosed using polysomnography in combination with respiratory and/or cardiovascular data (heart rate [46] and blood pressure [47]), and conventional hypnograms alone are often considered ineffective in determining OSA severity [46]. In this letter, we introduce a method to estimate the OSA severity through a physiological parameter L that is derived solely from standard hypnograms (fig. 4). More specifically, we have analyzed sleep data from healthy children and children with OSA, and we show that N1 sleep bout durations (Δt_{N1}) can be described by an exponential distribution with higher characteristic time constant for OSA children. We suggest a random-walk model to simulate the exponential distribution of Δt_{N1} by introducing a light sleep threshold L that distinguishes between more shallow and deeper light sleep. Using this model framework and the characteristics of a Wiener process, we can calculate L from the sleep data and find significantly higher L values for OSA compared to healthy children, which might explain the longer time OSA patients spend in light sleep N1. Moreover, we demonstrate that L correlates well with OSA severity, showing highest correlation

values for children with the most severe Obstructive Apnea Index (OAI).

OSA is characterized by repeated episodes of upper airway obstruction during sleep, which can result in intermittent brain hypoxia and sleep disruptions. Epochs of intermittent hypoxia can cause cellular injury in various parts of the central nervous system [48]. Because remote brain regions (at the edge of major vascular supply) are more susceptible to hypoxia, the cerebral cortex is particularly vulnerable [49]. Therefore, in OSA patients the hypoxic damage may lead to cortical dysfunctions causing some degree of cognitive impairments in attention, learning, and motor performance, which may lead to a growth deficit and abnormal behavior in children [50]. Since most of these impairments are partially reversible with OSA treatment [51], early diagnosis is crucial, especially for young children. Our results suggest that the parameter L , which we propose and develop in this letter, could be used as a new diagnostic marker for OSA since it captures the sleep microarchitecture, and therefore complements ODI which measures breathing disturbances. The estimation of L can easily be incorporated into clinical studies since it is derived from standard hypnograms and does not require additional equipment.

Further studies are needed to evaluate the diagnostic significance of L on a larger cohort of OSA patients that also include different age groups of the adult population as well as different types of OSA treatment. Another important problem is to study the applicability of L for other sleep disorders, for example, central sleep apnea (CSA) [52] that, in contrast to OSA, is caused by absent respiratory drive from the brain stem [19]. Although more research is needed to find the exact physiological explanation of L , this parameter could already be used in sleep apnea diagnostics.

* * *

This research was supported by the Bar-Ilan University and the Planning and Budgeting Committee fellowship program of the council for higher education of Israel; Shulamit Aloni Fellowship for Advancing Women in Exact Sciences and Engineering, Ministry of Science and Technology, Israel (Grant No. 3-13276); the Colman-Soref Grant foundation Fellowship of the Council for Higher Education, Israel (Grant No. kra/colman/194); the Israel Science Foundation (Grant No. 1657/16); the German Israeli Foundation (Grant No. I-1372-303.7/2016).

REFERENCES

- [1] LO C.-C., AMARAL L. N., HAVLIN S., IVANOV P. CH., PENZEL T., PETER J.-H. and STANLEY H. E., *Europhys. Lett.*, **57** (2002) 625.
- [2] CARSKADON M. A., DEMENT W. C. *et al.*, *Princ. Pract. Sleep Med.*, **4** (2005) 13.
- [3] ACHERMANN P., DIJK D.-J., BRUNNER D. P. and BORBÉLY A. A., *Brain Res. Bull.*, **31** (1993) 97.
- [4] ACHERMANN P. and BORBÉLY A. A., *Biol. Cybern.*, **71** (1994) 115.
- [5] ACHERMANN P. and BORBÉLY A. A., *Front. Biosci.*, **8** (2003) S683.
- [6] BEST J., DINIZ BEHN C., POE G. R. and BOOTH V., *J. Biol. Rhythms*, **22** (2007) 220.
- [7] BORBÉLY A. A. and ACHERMANN P., *J. Biol. Rhythms*, **14** (1999) 559.
- [8] REMPE M. J., BEST J. and TERMAN D., *J. Math. Biol.*, **60** (2010) 615.
- [9] LU J., SHERMAN D., DEVOR M. and SAPER C. B., *Nature*, **441** (2006) 589.
- [10] SAPER C. B., SCAMMELL T. E. and LU J., *Nature*, **437** (2005) 1257.
- [11] LO C.-C., BARTSCH R. P. and IVANOV P. C., *EPL*, **102** (2013) 10008.
- [12] DVIR H., ELBAZ I., HAVLIN S., APPELBAUM L., IVANOV P. CH. and BARTSCH R. P., *Sci. Adv.*, **4** (2018) eaar6277.
- [13] LO C.-C., CHOU T., PENZEL T., SCAMMELL T. E., STRECKER R. E., STANLEY H. E. and IVANOV P. CH., *Proc. Natl. Acad. Sci. U.S.A.*, **101** (2004) 17545.
- [14] BLUMBERG M. S., SEELKE A. M., LOWEN S. B. *et al.*, *Proc. Natl. Acad. Sci. U.S.A.*, **102** (2005) 14860.
- [15] BLUMBERG M. S., COLEMAN C. M., JOHNSON E. D. and SHAW C., *Eur. J. Neurosci.*, **25** (2007) 512.
- [16] DVIR H., KANTELHARDT J. W., ZINKHAN M., PILLMANN F., SZENTKIRALYI A., OBST A., AHRENS W. and BARTSCH R. P., *Biophys. J.*, **117** (2019) 987.
- [17] SILBER M. H., ANCOLI-ISRAEL S., BONNET M. H., CHOKROVERTY S., GRIGG-DAMBERGER M. M., HIRSHKOWITZ M., KAPEN S., KEENAN S. A., KRYGER M. H., PENZEL T., PRESSMAN M. R. and IBER C., *J. Clin. Sleep Med.*, **3** (2007) 121.
- [18] ROPPER A. H., SAMUELS M. A. and KLEIN J. P., *Sleep and Its Abnormalities*, in *Adams and Victor's Principles of Neurology* (The McGraw-Hill Companies, New York, NY) 2014, Chapt. 19.
- [19] SCAMMELL T. E., SAPER C. B. and CZEISLER C. A., *Sleep Disorders* (McGraw-Hill Education, New York, NY) 2018.
- [20] GENZEL L., KROES M. C., DRESLER M. and BATTAGLIA F. P., *Trends Neurosci.*, **37** (2014) 10.
- [21] PENZEL T., MÖLLER M., BECKER H. F., KNAACK L. and PETER J.-H., *Sleep*, **24** (2001) 90.
- [22] SCHUMANN A. Y., BARTSCH R. P., PENZEL T., IVANOV P. C. and KANTELHARDT J. W., *Sleep*, **33** (2010) 943.
- [23] SONG Y., BLACKWELL T., YAFFE K., ANCOLI-ISRAEL S., REDLINE S. and STONE K. L., *Sleep*, **38** (2015) 411.
- [24] HABA-RUBIO J., MARTI-SOLER H., TOBBACK N., ANDRIES D., MARQUES-VIDAL P., WAEBER G., VOLLENWEIDER P., VON GUNTEN A., PREISIG M., CASTELAO E. *et al.*, *Neurology*, **88** (2017) 463.
- [25] RATNAVADIVEL R., CHAU N., STADLER D., YEO A., McEVOY R. D. and CATCHESIDE P. G., *J. Clin. Sleep Med.*, **5** (2009) 519.
- [26] SCHLEMMER A., PARLITZ U., LUTHER S., WESSEL N. and PENZEL T., *Philos. Trans. R. Soc. A: Math. Phys. Eng. Sci.*, **373** (2015) 20140093.
- [27] HARRINGTON J., SCHRAMM P. J., DAVIES C. R. and LEE-CHIONG T. L., *Sleep Breath.*, **17** (2013) 1071.

- [28] MIANO S., PAOLINO M. C., CASTALDO R. and VILLA M. P., *Clin. Neurophysiol.*, **121** (2010) 39.
- [29] ZHU Y., AU C.-T., LAM H. S., CHAN C.-C. K., HO C., WING Y.-K. and LI A. M., *Sleep Med.*, **15** (2014) 303.
- [30] WELLMAN A. and REDLINE S., *Sleep Apnea* (McGraw-Hill Education, New York, NY) 2018.
- [31] CHERVIN R. D. and ARCHBOLD K. H., *Sleep*, **24** (2001) 313.
- [32] GOZAL D., *Pediatrics*, **102** (1998) 616.
- [33] GOZAL D. and POPE D. W., *Pediatrics*, **107** (2001) 1394.
- [34] SHELDON S. H., FERBER R. and KRYGER M. H., *Principles and Practice of Pediatric Sleep Medicine* (Elsevier Health Sciences) 2005.
- [35] GUILLEMINAULT C., WINKLE R., KOROBKIN R. and SIMMONS B., *Eur. J. Pediatr.*, **139** (1982) 165.
- [36] WEBER F. and DAN Y., *Nature*, **538** (2016) 51.
- [37] CHOU T. C., BJORKUM A. A., GAUS S. E., LU J., SCAMMELL T. E. and SAPER C. B., *J. Neurosci.*, **22** (2002) 977.
- [38] SAPER C. B., FULLER P. M., PEDERSEN N. P., LU J. and SCAMMELL T. E., *Neuron*, **68** (2010) 1023.
- [39] CLAUSET A., SHALIZI C. R. and NEWMAN M. E., *SIAM Rev.*, **51** (2009) 661.
- [40] LEON-GARCIA A., *Probability, Statistics, and Random Processes for Electrical Engineering* (Pearson Education) 2008.
- [41] EDWARDS A. M., PHILLIPS R. A., WATKINS N. W., FREEMAN M. P., MURPHY E. J., AFANASYEV V., BULDYREV S. V., DA LUZ M. G., RAPOSO E. P., STANLEY H. E. *et al.*, *Nature*, **449** (2007) 1044.
- [42] GALE S. D. and HOPKINS R. O., *J. Int. Neuropsychol. Soc.*, **10** (2004) 60.
- [43] CHUNG F., LIAO P., ELSAID H., ISLAM S., SHAPIRO C. M. and SUN Y., *Anesth. Analg.*, **114** (2012) 993.
- [44] TEMIRBEKOV D., GÜNEŞ S., YAZICI Z. M. and SAYIN İ., *Turk. Arch. Otorhinolaryngol.*, **56** (2018) 1.
- [45] GOLDSTEIN N. A., *Evaluation and Management of Pediatric Obstructive Sleep Apnea*, in *Cummings Pediatric Otolaryngology* (Elsevier, Philadelphia) 2015, pp. 45–54.
- [46] MA Y., SUN S., ZHANG M., GUO D., LIU A. R., WEI Y. and PENG C.-K., *Sleep Breath.*, **24** (2019) 231.
- [47] CAMARGO S., RIEDL M., ANTENEODO C., KURTHS J., PENZEL T. and WESSEL N., *PLoS ONE*, **9** (2014) e107581.
- [48] BEEBE D. W. and GOZAL D., *J. Sleep Res.*, **11** (2002) 1.
- [49] LEARY M. C., VELUZ J. S. and CAPLAN L. R., *Cerebrovascular Disease and Neurologic Manifestations of Heart Disease* (McGraw-Hill Education, New York, NY) 2017.
- [50] CHAN J., EDMAN J. C., KOLTAI P. J. *et al.*, *Am. Fam. Physician*, **69** (2004) 1147.
- [51] FERINI-STRAMBI L., BAIETTO C., DI GIOIA M., CASTALDI P., CASTRONOVO C., ZUCCONI M. and CAPPAS S., *Brain Res. Bull.*, **61** (2003) 87.
- [52] DVIR H., GUO S., HAVLIN S., XIN N., JUN T., LI D., ZHIFEI X., KANG R. and BARTSCH R. P., to be published in *IEEE Trans. Biomed. Eng.*, <https://www.doi.org/10.1109/TBME.2020.2979287>.